



**69th Annual
Scientific Conference**

Indianapolis

Indiana, USA

**AAAM 69th Annual Conference
Student Symposium
Abstracts**

**October 7-10, 2025
Indianapolis, Indiana, USA**

Effects of Legislative and Non-legislative Interventions on Child Occupant Crash Injuries in the United Arab Emirates

Muhammad Uba Abdulazeez, Kassim Abdullah
 Emirates Center for Mobility Research, United Arab Emirates University

Sjaan Koppel
 Monash University Accident Research Center, Monash University

INTRODUCTION

Road traffic crashes (RTCs) are the leading cause of morbidity and mortality for children aged 0-14 years in the United Arab Emirates (UAE) (Abdullah, Mourad, & Muhammad, 2020). Child vehicle occupants represent the majority of children injured due to RTCs in the UAE (Abdullah, Abdulazeez, & Mourad, 2022). Several child occupant safety initiatives have been launched in the UAE from 2010 onwards. These include promotional activities, media outreach, training programs, awareness initiatives, and educational campaigns. Additionally, free child safety seats (CSS) have been distributed to thousands of families with a child or those expecting a baby (Bromfield & Mahmoud, 2017; Grivna et al., 2012).

In 2007, child occupant safety legislation was introduced in the UAE mandating the use of CSS for children aged 0-4 years and seatbelts for children aged 5 and older, with the aim of improving child occupant safety (UAE Ministry of Interior, 2017). However, no study has evaluated the effects of these initiatives on reducing child occupant injuries in the UAE. Therefore, this study aimed to examine the effects of these interventions on reducing child occupant road traffic injuries (RTIs) for children aged 0-14 years.

METHODS

Child RTI data was obtained from the UAE Ministry of Interior for a twelve-year period (2012-2023). Additionally, data on the child population and crash incidence were sourced from the UAE Federal Competitiveness and Statistics Authority.

The outcome variables were the percentage changes in the rates of minor, moderate, severe, and fatal RTIs from 2012 to 2023. The rates were computed per 100,000 child population and per 1,000 number of crashes. These rates were calculated per 100,000 child population to reflect health risk and per 1,000

crashes to indicate traffic exposure risk (Nazif-Munoz & Nikolic, 2018).

RESULTS

Table 1 presents the percentage changes in RTI rates for child occupants aged 0-4 years from 2012 to 2023. Per 100,000 child population, the rate of fatal injuries decreased by 100% while minor injuries increased by 2%, moderate injuries by 40%, and severe injuries by 131% in 2023 compared to 2012. When calculated per 1,000 crashes, the rates of minor, moderate, and severe injuries decreased by 67%, 54%, and 24% respectively, with fatal injuries also decreasing by 100%.

Table 1. RTI rate changes for children 0-4 years

| Injury severity | Injuries per 100000 population | | | Injuries per 1000 crashes | | |
|-----------------|--------------------------------|-------|----------|---------------------------|-------|----------|
| | 2012 | 2023 | % change | 2012 | 2023 | % change |
| Minor | 22.55 | 22.90 | +0.02 | 217.57 | 72.06 | -0.67 |
| Moderate | 7.13 | 9.96 | +0.40 | 68.85 | 31.33 | -0.54 |
| Severe | 0.86 | 1.99 | +1.31 | 8.26 | 6.27 | -0.24 |
| Fatal | 1.43 | 0.00 | -1.00 | 13.77 | 0.00 | -1.00 |

Table 2. RTI rate changes for children 5-9 years

| Injury severity | Injuries per 100000 population | | | Injuries per 1000 crashes | | |
|-----------------|--------------------------------|-------|----------|---------------------------|-------|----------|
| | 2012 | 2023 | % change | 2012 | 2023 | % change |
| Minor | 31.35 | 11.59 | -0.63 | 212.06 | 81.45 | -0.62 |
| Moderate | 16.69 | 10.25 | -0.39 | 112.92 | 72.06 | -0.36 |
| Severe | 4.07 | 4.01 | -0.01 | 27.54 | 28.20 | +0.02 |
| Fatal | 2.04 | 3.12 | +0.53 | 13.77 | 21.93 | +0.59 |

Table 3. RTI rate changes for children 10-14 years

| Injury severity | Injuries per 100000 population | | | Injuries per 1000 crashes | | |
|-----------------|--------------------------------|-------|----------|---------------------------|--------|----------|
| | 2012 | 2023 | % change | 2012 | 2023 | % change |
| Minor | 26.59 | 10.42 | -0.61 | 184.52 | 106.52 | -0.42 |
| Moderate | 26.59 | 11.34 | -0.57 | 184.52 | 115.91 | -0.37 |
| Severe | 4.76 | 1.84 | -0.61 | 33.05 | 18.8 | -0.43 |
| Fatal | 1.19 | 0.00 | -1.00 | 8.26 | 0.00 | -1.00 |

Table 2 presents the changes in child occupant RTI rates for children aged 5-9 years. Per 100,000 child population, moderate and severe injury rates decreased by 39% and 1% respectively while minor and fatal injury rates increased by 63% and 53% respectively. When calculated per 1,000 crashes, severe and fatal injury rates increased by 2% and 59% respectively whereas minor and moderate injury rates declined by 62% and 36% respectively.

Table 3 displays the changes in child occupant RTI rates for children aged 10-14 years. Per 100,000 child population, the rates of minor, moderate, and severe injuries decreased by 61%, 57%, and 61% respectively with fatal injuries declining by 100%. Similarly, per 1,000 crashes, the rates of minor, moderate, and severe injuries fell by 42%, 37%, and 43% respectively with a 100% reduction in fatal injuries.

DISCUSSION

This is the first study to evaluate the impact of child occupant safety legislative and non-legislative interventions on child occupant RTIs in the UAE. The current findings showed mixed effects of these interventions on child occupant RTI reduction. While the interventions were successful in achieving comprehensive reductions in child occupant RTI rates for children aged 10-14 years, their effectiveness in reducing the RTI rates for children aged 0-4 years and 5-9 years was less pronounced.

The interventions were effective in reducing the traffic exposure risk for all the injury severity levels and the health risk for fatal injuries while they were ineffective in reducing the health risk for minor, moderate, severe, and fatal injuries for children aged 0-4 years. Most of the non-legislative interventions on CSS use have been observed to be replicas of similar interventions adopted in western countries and are less effective in the UAE due to cultural and societal norms (Bromfield & Mahmoud, 2017). Therefore, culturally appropriate interventions that are more persuasive should be developed and implemented to achieve comprehensive reductions in the health risks of RTIs for children in this age group.

In the UAE, children aged 0-4 years are legally required to use CSS while travelling in vehicles. However, the law does not specify the appropriate type of CSS based on a child's age, weight, or height. This lack of guidance may lead to inappropriate CSS selection and use, potentially compromising the effectiveness of the CSS. Inappropriate CSS use significantly increases the risk of injury to child occupants (Durbin, Elliott, & Winston, 2003).

Therefore, enhanced legislation is needed aligned with best practice recommendations to clearly define the appropriate type of CSS required for child occupants in the UAE, ensuring optimal protection and safety.

The child occupant safety interventions were observed to result in reducing both the health and traffic exposure risks of minor and moderate injuries as well as the health risk of severe injuries while they were ineffective in reducing both the health and traffic exposure risks of fatal injuries and the traffic exposure risk of severe injuries for children aged 5-9 years. Children in this age group can be legally restrained by an adult seatbelt in the UAE. However, vehicle seatbelts are designed for adults and do not adequately protect children (Brolin et al., 2015). This could be the reason for the increased traffic exposure risks of severe and fatal injuries as well as the health risk of fatal injuries.

Research has shown that children in this age group who are restrained using an adult seatbelt are highly susceptible to severe abdominal-related injuries (Hu et al., 2013; Ouyang et al., 2015), spinal fractures (Durbin et al., 2018; Fadl & Sandstrom, 2019), and head injuries in frontal crashes (Bohman et al., 2011). On the other hand, booster seats have been demonstrated to offer enhanced protection for children in this age group (Mannix et al., 2012). Hence, enhanced (booster seat) legislation is required to adequately protect children in this age group while travelling in a motor vehicle.

A study evaluating the effectiveness of child occupant legislation in Serbia which mandated the use of CSS for children aged 0-3 years and seatbelt use for children aged 4-12 years found that the intervention was more effective in reducing injuries for the older age group (4-12 years) compared to the younger age group (0-3 years) (Nazif-Munoz & Nikolic, 2018). The authors attributed this finding to the presence of seatbelts in the rear seats of all vehicles, thereby facilitating their immediate use by the children. This explanation may also help account for the findings of the current study, specifically the substantial reductions observed in both health-related and traffic exposure injury risks for children aged 10-14 years.

CONCLUSION

This is the first study to evaluate the impact of child occupant safety legislative and non-legislative interventions on child occupant RTIs in the UAE. The study findings revealed mixed outcomes regarding the impacts of these interventions on

reducing child occupant RTIs. While the interventions led to significant reductions in injury risks for children aged 10-14 years, their effectiveness was less evident for younger age groups, specifically child occupants aged 0-4 and 5-9 years.

NOVELTY/TRAFFIC SAFETY IMPLICATIONS

The current findings indicate that while child occupant safety interventions in the UAE have been effective in reducing traffic exposure risks associated with RTIs, further efforts are needed to achieve substantial reductions in the health-related RTI risks of RTIs particularly among child occupants aged 0-9 years.

ACKNOWLEDGEMENTS

This study was sponsored by the United Arab Emirates University's Research and Sponsored Projects Office with Grant No: 31N378.

REFERENCES

Abdullah, K. A., Abdulazeez, M. U., & Mourad, A. H. I. (2022). Characterizing Child Occupant Crash Injuries in United Arab Emirates. *2022 Advances in Science and Engineering Technology International Conferences (ASET)* (pp. 1–6). IEEE.

Abdullah, K. A., Mourad, A. H. I., & Muhammad, A. U. (2020). Child Passenger Safety in the United Arab Emirates: A Review. *2020 Advances in Science and Engineering Technology International Conferences (ASET)* (pp. 1–6). IEEE.

Bohman, K., Stockman, I., Jakobsson, L., Osvalder, A.-L., Bostrom, O., & Arbogast, K. B. (2011). Kinematics and shoulder belt position of child rear seat passengers during vehicle maneuvers. *Annals of Advances in Automotive Medicine/Annual Scientific Conference* (Vol. 55, p. 15). Association for the Advancement of Automotive Medicine.

Brolin, K., Stockman, I., Andersson, M., Bohman, K., Gras, L.-L., & Jakobsson, L. (2015). Safety of children in cars: A review of biomechanical aspects and human body models. *IATSS research*, *38*(2), 92–102. Elsevier.

Bromfield, N., & Mahmoud, M. (2017). An exploratory investigation of child safety seat use among citizens of the United Arab Emirates. *Journal of Transportation Safety & Security*, *9*(sup1), 130–148. Taylor & Francis.

Durbin, D. R., Elliott, M. R., & Winston, F. K. (2003). Belt-positioning booster seats and reduction in risk of injury among children in vehicle crashes. *Jama*, *289*(21), 2835–2840. American Medical Association.

Durbin, D. R., Hoffman, B. D., Agran, P. F., Denny, S. A., Hirsh, M., Johnston, B., Lee, L. K., et al. (2018). Child passenger safety. *Pediatrics*, *142*(5). American Academy of Pediatrics.

Fadl, S. A., & Sandstrom, C. K. (2019). Pattern recognition: a mechanism-based approach to injury detection after motor vehicle collisions. *RadioGraphics*, *39*(3), 857–876. Radiological Society of North America.

Grivna, M., Aw, T.-C., El-Sadig, M., Loney, T., Sharif, A. A., Thomsen, J., Mauzi, M., et al. (2012). The legal framework and initiatives for promoting safety in the United Arab Emirates. *International journal of injury control and safety promotion*, *19*(3), 278–289. Taylor & Francis.

Hu, J., Wu, J., Reed, M. P., Klinich, K. D., & Cao, L. (2013). Rear seat restraint system optimization for older children in frontal crashes. *Traffic injury prevention*, *14*(6), 614–622. Taylor & Francis.

Interior, U. M. of. (2017). New UAE Traffic Law Comes into Force. *UAE Government*. Retrieved December 14, 2019, from <https://www.government.ae/en/information-and-services/justice-safety-and-the-law/road-safety>

Mannix, R., Fleegler, E., Meehan III, W. P., Schutzman, S. A., Hennelly, K., Nigrovic, L., & Lee, L. K. (2012). Booster seat laws and fatalities in children 4 to 7 years of age. *Pediatrics*, *130*(6), 996–1002. American Academy of Pediatrics Elk Grove Village, IL, USA.

Nazif-Munoz, J. I., & Nikolic, N. (2018). The effectiveness of child restraint and seat belt legislation in reducing child injuries: The case of Serbia. *Traffic injury prevention*, *19*(sup1), S7–S14. Taylor & Francis.

Ouyang, J., Zhu, Q., Zhong, S., Li, Z., & Liu, C. (2015). Abdominal impact study on paediatric cadaveric subjects. *International journal of vehicle safety*, *8*(4), 287–298. Inderscience Publishers (IEL).

Predicting Severe Motorcycle Crashes using Motorcycle Crash Causation Study Narratives

L. Garrett Bangert, Divya Polavarapu, Caitlyn. J. Collins

Virginia Tech

Introduction - Motorcycles are overrepresented in motor vehicle crashes, accounting for only 3% of the vehicle fleet but 14% of the total crashes in the US (NHTSA 2023, Preusser 1995). Furthermore, motorcycle crashes more often result in serious and fatal injuries, with motorcyclists at a 37-times greater risk of sustaining a fatal injury compared to passenger vehicle occupants (NHTSA 2008). Studying the cause of motorcycle crashes is difficult due to the lack of descriptive data, but previous analyses have attempted to identify causal factors of motorcycle crashes using data from in-depth investigations of the crash. These studies have identified important factors associated with severity, such as rider skill and behavior (Bucshazy 2020), vehicle characteristics (Chand 2021), and environmental perceptions (Islam 2021); however, these models are limited to tabular data and can miss causal insights hidden in unstructured text data from the crash narratives collected on-site. Recently, predictive models of crash severity using regression (Chawla 2019, Wali 2019) and machine learning (Arteaga 2020) have analyzed text data taken directly from crash narratives to inform traffic safety policy by discovering latent topics, or hidden themes that can be implied from recurring themes in a group of similar narratives. Training predictive models of crash outcomes using text data is an emerging area of research, and insights from discovered latent topics can identify factors not captured in tabular data or police reports (Das 2021).

Machine learning (ML) and Natural Language Processing (NLP) are emerging tools used to leverage latent topics from crash narratives to predict crash outcomes. One example is from Janstrup et al., 2023 that predicted emergency services response to bicycle crashes using a neural network (NN) trained on latent topics from self-report narratives. A popular technique to establish latent topics is called Latent Dirichlet Allocation (LDA), an unsupervised clustering algorithm that groups documents based on similar hidden themes between documents. Furthermore, Janstrup et al. used SHapley Additive exPlanations (SHAP) to address issues of interpretability associated with ML. SHAP is a useful technique for explaining how training features contributed to specific ML predictions, i.e., which factors increased the probability of higher severity predictions. Using these

techniques, Janstrup et al. linked latent topics with emergency response behaviors, e.g., school zones and heavy traffic were found to increase the probability that an ambulance drove fast with a siren.

Natural language processing and data-driven modeling tools have the potential to identify overlooked causal factors, providing new insights for traffic safety policy and injury countermeasures. Few studies have implemented NLP and ML to predict crash outcomes utilizing data rich textual descriptions of causal factors contributing to motorcycle crashes. Therefore, the goal of this study is to predict motorcycle crash severity using latent topics derived from detailed crash narratives to train a NN classification model.

Methods – The narratives of motorcycle crashes were identified from the Motorcycle Crash Causation Study (MCCS) (NHTSA 2019). MCCS is a large-scale case-control study containing data from in-depth crash investigations. MCCS reports include textual descriptions of the crash situation, crash type, and human, vehicle, and environmental factors relevant to the cause of a crash.

Topic Modelling

MCCS crash narratives were preprocessed using a variety of important NLP techniques used in previous studies (Khurana 2022). First, HTML characters and punctuation were dropped, and characters were converted to lowercase. A spellcheck was conducted and numerical characters were replaced with text, e.g., “2” is replaced by “two”. Next, negative words, such as “no” and “not”, were concatenated with the following word to form phrases like “no_crash” and “no_vehicle”. Next, all words were abbreviated to their lemma, or the meaningful part a word; a process known as lemmatization. Specific words, known as stop words, were also removed since these words add no meaning or context such as “and” or “the”. As in Arteaga 2020, removing words that are unhelpful to the classification task can reduce model accuracy, but result in more meaningful explanations. Accordingly, words like “however” and “causation” were removed as they occurred in the majority of crash narratives.

The NLP-processed crash narratives were converted to collections of meaningful words, and a dictionary, or corpus, of these meaningful words was generated using the Bag-of-Words model where the frequency of each word in narratives is computed and assigned a unique identifier. Next, LDA was used to group narratives into an optimized number of topics using the maximum normalized coherence and minimum perplexity score as described in Hasan et al, 2021. Here, coherence refers to the logical structure of narratives belonging to the same topic, and perplexity refers to how well a model can predict which topic a narrative belongs to. High coherence indicates similarity between the themes of documents within a topic have, and low perplexity indicates the model can easily predict the topic a narrative belongs to. The result of LDA is a probability from 0 to 1 of how likely a narrative belongs to each of the generated topics and were the only features used to train the NN in this study to predict motorcycle crash severity.

Predict Injury Severity – Crash injury severity is often represented by the Abbreviated Injury Scale (AIS), which categorizes the severity of each injury an occupant sustained where AIS 1 is a minor injury and AIS 6 is an untreatable injury (Gennarelli 2016).

The Injury Severity Score (ISS) is another anatomical injury scoring system correlated with mortality and other important measures of injury severity. ISS is scored on a scale of 0 to 75 and is determined by summing the most severe injuries determined by the Abbreviated Injury Scale (AIS) in the 3 most severely injured body regions. This study developed a supervised NN model to predict whether a M CCS case resulted in severe injuries using the topic probabilities from LDA. Severe crashes were defined as cases with ISS 12+ like Hung et al. (2021), which implies an occupant suffered at least 2 moderate or serious injuries. M CCS cases with an unknown ISS were excluded from this analysis, resulting in a selection of 342 of the total 351 cases. The NN structure was developed based on Janstrup et al. 2023, which used a simple sequential model of an input layer, a hidden layer, and a dense output layer. The optimal number of these layers, number of nodes within each layer, and the learning rate used in this model were determined via Bayesian hyperparameter tuning, and the sigmoid activation function was used for binary classification of crash outcomes. 5-fold cross validation was used to incorporate all M CCS cases in the training and validation steps, reducing issues of overfitting. Finally, SHAP was used to explain how latent topics influenced the NN predictions of crash severity, and a qualitative analysis of the most common topical

themes associated with increased prediction of higher severity was performed.

Results – Based on the optimal selection of normalized coherence and perplexity values, the number of topics was set to 9 (Figure 1). **Normalized Perplexity and Coherence**

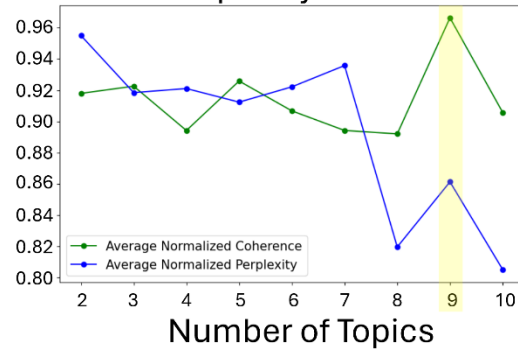


Figure 1. Coherence and perplexity of M CCS narratives for varying numbers of topics.

The optimized NN achieved an accuracy of 76.6% with an average loss over all folds of 0.58. Figure 2 summarizes the SHAP analysis of all M CCS narratives, indicating how each topic impacted the NN predictions of crash severity in all cases. Here, each data point represents the SHAP value associated with the probability that a M CCS case belongs to a topic. Red points indicate that a case had a high probability of belonging to that topic, and positive SHAP values indicate that the probability of belonging to that topic increased the probability of predicting an ISS 12+ outcome for a particular case.

SHAP Summary of LDA Topic Probabilities

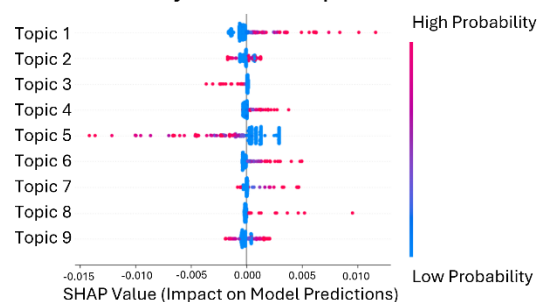


Figure 2. SHAP summary plot for the 9 Topics.

Topics are constituted of the recurring textual themes within the clustered narratives belonging to that topic. The top 10 recurring themes of narratives associated with Topics 6 and 7 are displayed in Figure 3 to provide an example of the insights achieved through the topic modeling in this study.

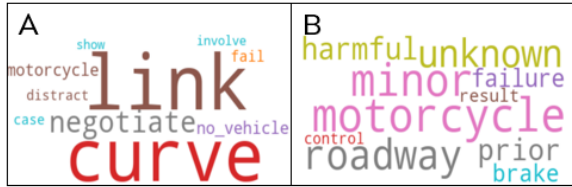


Figure 3. Frequent textual themes of documents in (A) Topic 6 and (B) Topic 7.

Discussion – The SHAP analysis in Figure 2 indicates that narratives belonging to Topics 1, 6, 7, and 8 were associated with increased probability of predicting a severe crash and that Topics 3 and 5 were associated with decreased probability of a severe crash. Topics 6 and 7 had a similar positive effect on the probability that the NN predicted an outcome of ISS 12+, and the recurring themes of these topics can be examined to discover what themes link narratives belonging to this topic. Themes such as “Negotiate”, “curve”, and “distract” were common in Topic 6, and “harmful”, “failure”, and “brake” were common in Topic 7 (Figure 3). Based on these themes, Topic 6 could be condensed to a label of “failure to negotiate curve”, and Topic 7 could be labeled “brake failure”. Das et al. 2021 previously conducted a topic modeling analysis using MCCS narratives and found that themes of “failure”, “unsafe speed”, and “intersection” were common in cases with fatal injuries. Specifically, “brake failure” was noted as contributing to fatal cases, which supports the association between increased probability NN predicting a severe crash and Topic 7 in this study. The themes of distraction and negotiating curves in Topic 6 were not noted in Das et al., possibly due to the difference in studying fatal crashes vs. crashes with an ISS of 12 or greater. A future direction that can impact safety policy is to analyze the geographic characteristics of cases belonging to Topic 6 to identify curved roads which are overrepresented in severe motorcycle crashes. Furthermore, future models can utilize both tabular and text data to study more complex relationships between crash narratives and characteristics of the crash event. The authors acknowledge some limitations within this study, namely the representation of MCCS data and binarization of crash severity. Future studies are needed to assess the distribution of demographics and crash types in MCCS cases compared with nationally representative datasets such as the National Automotive Sampling System dataset using robust statistical design. Finally, the binarization of injury severity implies that all cases with ISS 12 through 75 are the same. Future studies can expand on the complexity of this categorization by using 3 or more categories of injury severity, such as isolating fatal crashes.

Conclusion – To the knowledge of the authors, this is the first implementation of a NN to predict motorcycle

crash severity using MCCS text data from crash narratives. This study successfully predicted motorcycle crash severity with a NN trained using the discovered latent topics in MCCS crash narratives alone. SHAP explanations indicated which topics increased the probability that the NN predicted an outcome of ISS 12+; some frequently occurring themes in topics associated with increased crash severity were negotiating a curve, brake failure, and distraction. Future directions include studying more complex categorizations of injury severity, identifying geographic-specific factors of crash severity, and examining the representation of MCCS data.

REFERENCES

- A. Chand, et al., “Road traffic accidents: An overview of data sources and contributing factors,” *Materials Today*, Jan. 2021
- B. Wali et al., “Examining Correlations between Motorcyclists Conspicuity, Apparel Related Factors and Injury Severity Score: Evidence from New Motorcycle Crash Causation Study. *Accident Analysis and Prevention*, 2019
- C. Arteaga, et al., “Injury severity on traffic crashes: A text mining with an interpretable approach,” *Safety Science*, Dec 2020
- D. F. Preusser, et al., “Analysis of fatal motorcycle crashes: crash typing,” *Accident Analysis & Prevention*, Dec. 1995
- H. Chawla et al., “Contrasting Crash- and Non-Crash Involved Riders: Analysis of Data from the Motorcycle Crash Causation Study. *Transportation Research Record: Journal of Transportation Research Board*, 2019
- K. Bucsházy, et al., “Human factors contributing to the road traffic accident occurrence,” *Transportation Research Procedia*, Jan. 2020
- K. H. Janstrup, et al., “Predicting injury-severity for cyclist crashes using natural language processing and neural network modelling,” *Safety Science*, 2023
- K. Hung et al., “Impacts of injury severity on long-term outcomes following motor vehicle crashes,” *BMC Public Health*, Mar. 2021
- M. Hasan et al., “Normalized Approach to Find Optimal Number of Topics in LDA,” *Computational Engineering*, 2021
- M. Islam, “The effect of motorcyclists’ age on injury severities in single-motorcycle crashes with unobserved heterogeneity,” *Journal of Safety Research*, Jun. 2021
- NHTSA, “Traffic Safety Facts - Motorcycle Helmet Use Laws,” DOT HS 810 887W, 2008.
- NHTSA. National Center for Statistics and Analysis, “Traffic Safety Facts 2021:” DOT HS 813 527, Dec. 2023.
- NHTSA, “Motorcycle Crash Causation Study: Final Report”, February 2019 - FHWA-HRT-18-064.
- S. Das et al., “Topic Models from Crash Narrative Reports of Motorcycle Crash Causation Study”, *Transportation Research Record*, 2021.
- T. Gennarelli, & e. Woodzin, Eds., 2016. *Association for the Advancement of Automotive Medicine, Abbreviated Injury Scale (c) 2005 Update 2008.*

Proactive Crash Risk Detection Through Community-Reported Concerns & Near Misses: A Network-Based Spatial Analysis

Katarina Cook, MS
UC Davis School of Medicine

INTRODUCTION

Between 2015 and 2024, Sacramento consistently experienced the highest per capita rates of automobile crashes and fatalities among major cities in California (TIMS, 2025). In response to increasing road injuries and fatalities, Sacramento declared a state of emergency in late 2024, underscoring the urgent need for improved crash prevention strategies.

Traditional crash analyses often overlook near-misses, incidents where crashes narrowly avoid occurring, despite their potential as early indicators of unsafe conditions (Heinrich, 1931; Perkins & Harris, 1968). Recent studies have demonstrated that integrating near-miss data with crash records can better identify high-risk locations and inform proactive interventions (Xu et al., 2024; Park et al., 2023; Aldred & Crosweiler, 2015). However, these approaches typically rely on automated detection methods, such as sensors or camera systems, which can limit input from communities directly experiencing traffic hazards (Chung et al., 2013).

This study employs resident-reported near-miss data, using spatial network analysis methods including the network-based K- and G-functions to determine whether near-miss complaints spatially cluster with police and municipality reported crash sites in Sacramento (Okabe & Yamada, 2001). Aligning with the Safe System approach, which prioritizes upstream and systems-level interventions to prevent injury (Ederer et al., 2023), this analysis highlights the potential of community-sourced data in guiding targeted, proactive safety improvements.

METHODS

Data Collection and Preprocessing

Near-miss reports were collected via community surveys distributed to Sacramento neighborhood organizations from November 2024 to March 2025. Each submission included coordinates, free-text descriptions, and categorical concern tags. Entries classified as "Other" were manually reclassified into predefined categories. Reports (n=234) were geocoded (WGS84), with 24 excluded for falling outside city limits. Crash data (n=5091) within Sacramento city boundaries for 2023-2024 were

sourced from UC Berkeley's Transportation Injury Mapping System (TIMS), derived from CHP's Statewide Integrated Traffic Records System (SWITRS). Crashes on state highways were excluded. All spatial data were projected to NAD83 for accurate spatial operations.

Spatial Analysis

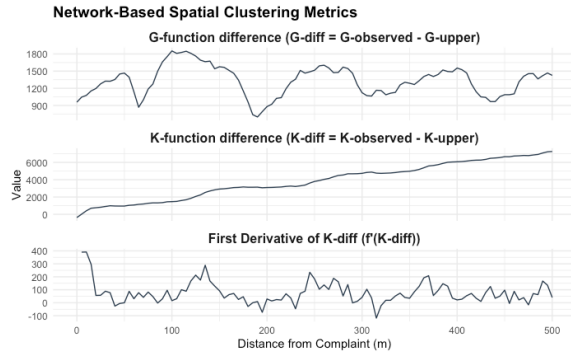
Spatial clustering between concern sites and crashes was assessed using network-constrained cross K- and G-functions. The street network from U.S. Census TIGER/Line shapefiles was segmented using R's spNetwork. Concern and crash locations were snapped to nearest network segments. Cross K-functions quantified cumulative clustering along the network, while G-functions assessed local crash densities at incremental bands (0–500 m, 5 m intervals). Monte Carlo simulations (99 iterations) generated 95% confidence envelopes to identify significant clustering.

Crash Aggregation, Severity and Typology

Spatial buffers at multiple distance bands identified from spatial analysis were applied around each concern site using R's sf package. Crashes within buffers were matched to the closest concern site buffer, prioritizing the smallest distance to avoid duplication; unmatched crashes fell outside all buffers. Crash severity and Healthy Places Index (HPI) percentiles were spatially joined to crash points. To assess whether types of concerns were associated with more severe crash outcomes, crashes matched to each complaint type under 150 m were stratified by injury severity (Fatal, Severe, Minor, and Possible Injury). Chi-square tests compared categorical severity distributions between buffer bands and unmatched sites, while Wilcoxon rank-sum tests assessed differences in continuous HPI scores.

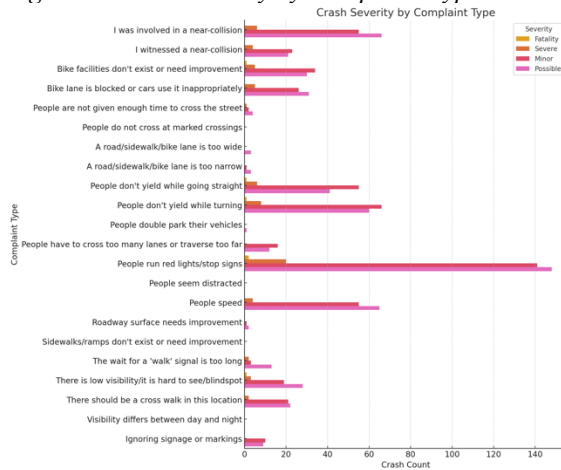
RESULTS

Figure 1: Network-Based Spatial Clustering Metrics



Spatial clustering analysis revealed multiple distances of significance for crash density near reported concern sites (Figure 1). A peak in the first derivative of the K-function difference (ΔK) was observed at 5 meters. The G-function difference (G-diff) reached an initial peak at 50 meters, followed by a trough. The most significant clustering based on G-diff was detected at 100 meters. A secondary peak in the K-function derivative appeared at 135 meters. Notably, the K-function continued to increase beyond 500 meters. Using these findings, buffer bands were applied at key distances of 5 m, 50 m, 100 m and 150 m from each concern site (Table 1).

Figure 2: Crash Severity by Complaint Type



“People run red lights/stop signs” had the highest number of total matched crashes ($n = 311$), and the highest number of severe injuries ($n = 20$) and fatalities ($n = 2$). “People don’t yield while turning” ($n = 135$) and “People speed” ($n = 124$) followed in total crash volume, with 8 and 4 severe injuries, respectively. “People don’t yield while going straight” ($n = 103$) and “I was involved in a near-collision” ($n = 127$) were also prominent. These differences did not reach statistical significance.

Table 1: Statistical Analysis Results for Key Distances from Complaint Sites

| | 0-5m | 6-50m | 51-100m | 101-150m | Not Near Complaint |
|----------------------------|-------------|-------------|-------------|-------------|--------------------|
| Count | 71 | 218 | 149 | 367 | 4286 |
| %All Crashes | 1.39 | 4.28 | 2.93 | 7.21 | 84.12 |
| χ^2 of Crash Severity | 1.79 | 1.90 | 2.70 | 2.21 | 3.75 |
| χ^2 P-value | 0.617 | 0.593 | 0.441 | 0.531 | 0.290 |
| Mean HPI Percentile | 68.9 | 68.4 | 65.1 | 62.2 | 39.3 |
| Wilcoxon P-value* | $p < 0.001$ | $p < 0.001$ | $p < 0.001$ | $p < 0.001$ | - |

*Each buffer zone compared to unmatched. No difference found between various buffer groups.

DISCUSSION

The primary aim of this study was to assess whether near-miss complaints are spatially clustered near crash sites more than would be expected under a random distribution on the street network. Network-based K- and G-function analyses confirmed that crash events are significantly clustered around concern sites across multiple distance thresholds, providing statistical support for the spatial validity of community-reported near-miss data.

By examining the first derivative of the K-function difference, I identified a clustering inflection point as close as 5 meters from reported concern sites. The G-function difference, which assesses local event proximity, showed an initial peak at 50 meters and its strongest peak at 100 meters, with a second inflection in ΔK at 135 meters. These findings suggest that the spatial association between crash incidents and concern sites is most concentrated within a 150-meter radius and begins as close as the width of a single intersection.

To translate these findings into practical assessment zones, I applied buffer bands at 0–5 m, 6–50 m, 51–100 m, and 101–150 m around each complaint site. Crashes within these proximity bands collectively accounted for over 15% of all recorded crashes. This reinforces the value of near miss reports as a tool for identifying locations of latent road danger. While crash severity did not differ significantly across buffer zones, certain complaint types, such as failure to yield, speeding, or signal violations, were more frequently associated with severe or fatal outcomes, suggesting a potential for complaints to signal not just location but also underlying crash mechanisms.

Assessing social determinants revealed a notable divergence: crashes within all buffer zones occurred in census tracts with significantly higher Healthy Places Index (HPI) percentiles compared to unmatched crashes. The HPI is a comprehensive metric of biosocial wellbeing, using 23 indicators of socioeconomic status, education, housing, transportation, environmental pollution, built environment, and health care access to summarize community conditions. This skewed distribution may reflect geographic reporting bias, where communities with greater resources, digital access, or civic infrastructure are more likely to submit near-miss reports. This discrepancy raises important considerations for incorporating public complaints into planning decisions, particularly in under-resourced areas where both crashes and unmet safety needs may be more prevalent.

CONCLUSION

These findings establish that community-reported near-miss data can reliably identify locations with higher-than-expected crash frequencies in a mid-sized California city, demonstrating value as a proactive tool for anticipating road safety risks. While near-miss complaints effectively pinpoint hazardous areas and crash mechanisms, such as speeding and yielding violations, they do not predict crash severity. An important limitation identified was the geographic bias in reporting, with complaint data disproportionately coming from higher-resourced neighborhoods. Addressing this imbalance through targeted outreach and engagement strategies will be crucial for fully leveraging community-reported data in equitable, proactive transportation safety planning.

NOVELTY/TRAFFIC SAFETY IMPLICATIONS

Significant clustering of community-reported near-miss complaints near documented crash highlights the potential of using low-cost, crowd-sourced data as an effective early-warning system to proactively identify and prioritize high-risk sites for targeted interventions. This approach can assist engineers in prioritizing infrastructure improvements, city planners in developing targeted interventions, and policymakers in crafting data-driven, equitable safety initiatives. From a public health perspective, this approach aims for upstream identification and prevention of motor vehicle injuries, reducing the burden on trauma and emergency care systems.

However, integrating these findings into equitable transportation safety practices requires deliberate outreach in historically underserved communities,

where underreporting may mask genuine safety risks. Otherwise, safety interventions risk reinforcing, rather than reducing, disparities in traffic injury and fatality outcomes.

ACKNOWLEDGEMENTS

This work was made possible by Isaac Gonzales and the energy that he has poured into Slow Down Sacramento to protect our neighbors.

REFERENCES

- Aldred R, Croweller S. Investigating the rates and impacts of near misses and related incidents among U.K. cyclists. *J Transp Health*. 2015;2(3):379-393. doi:10.1016/j.jth.2015.05.006
- Chung Y, Eom K, Won M. An Innovative Approach for Traffic Safety Improvement Based on Public Involvement via Social Network Services. The Korea Transport Institute; 2013.
- Ederer DJ, Panik RT, Botchwey N, Watkins K. The Safe Systems Pyramid: A new framework for traffic safety. *Transp Res Interdiscip Perspect*. 2023;21:100905. doi:10.1016/j.trip.2023.100905
- Heinrich HW. *Industrial Accident Prevention: A Scientific Approach*. McGraw-Hill; 1931.
- Okabe A, Yamada I. The K-function method on a network and its computational implementation. *Geogr Anal*. 2001;33(3):271-290. doi:10.1111/j.1538-4632.2001.tb00448.x
- Park JI, Kim S, Kim JK. Exploring spatial associations between near-miss and police-reported crashes: The Heinrich's law in traffic safety. *Transp Res Interdiscip Perspect*. 2023;19:100830. doi:10.1016/j.trip.2023.100830
- Perkins S, Harris J. Traffic conflict characteristics—accident potential at intersections. *Highw Res Rec*. 1968;225:35-43.
- Safe Transportation Research and Education Center (SafeTREC). *Transportation Injury Mapping System (TIMS)*. University of California, Berkeley; 2025.
- Xu C, Gao J, Zuo F, Ozbay K. Estimating urban traffic safety and analyzing spatial patterns through the integration of city-wide near-miss data: A New York City case study. *Appl Sci*. 2024;14(14):6378. doi:10.3390/app14146378

Burden of hospitalization for adolescent bicycling injuries: United States, 2016 – 2020

Amir Ghanbari ^{1,2}

1. Department of Epidemiology, University of Iowa, USA
2. Injury Prevention Research Center, University of Iowa, USA

Cara Hamann ^{1,2}

INTRODUCTION

Bicycling has gained widespread recognition as a sustainable, affordable, and health-promoting mode of transportation and recreation in the United States (CDC, 2022, Mueller et al., 2015). With expanding urban bicycling infrastructure and increasing interest in active transportation, national bicycling rates have grown across a broad demographic, including children, teens, and older adults (McGuckin & Fucci, 2018; PeopleForBikes, 2022). Although bicycling has clear physical and environmental benefits, it may also pose a significant risk of injury, particularly when sharing roads with motor vehicles or in poor infrastructure areas.

Bicycle-related injuries hospitalizations represent a serious public health burden. Bicycle crashes are estimated to cost more than \$23 billion each year, including medical care, lost productivity, and premature death. (CDC, 2022). Although the majority of injuries occur in outpatient or emergency settings (Sarmiento et al., 2021), more severe cases need inpatient care, reflecting greater injury severity, surgical intervention, or prolonged recovery. While there has been research documenting the burden of bicycling injuries (Hamann et al., 2013; Næss et al., 2020), a lack of focus remains on comparing these injuries' characteristics and outcomes between urban and rural settings. In a study conducted in the United States, bicycling injuries were stratified by motor vehicle involvement (MVC vs. non-MVC) and it was found that MVC-related injuries resulted in longer hospital stays, higher costs, and more non-routine discharges compared to injuries not caused by motor vehicles (Hamann et al., 2013). That analysis, now over a decade old, relied on ICD-9 coding and preceded major developments such as the adoption of ICD-10 and evolving road safety initiatives. While previous work has focused on crash mechanisms, less is known about how bicycling injuries vary by geographic context. To address this gap, the present study provides aims to update national estimates and overall burden of bicycle-related hospitalizations

using recent ICD-10 data, stratifying by crash location (urban vs. rural) to better understand population-level patterns and disparities.

METHODS

Data Source and Study Population

We conducted a cross-sectional analysis using the HCUP Nationwide Inpatient Sample (NIS) for the years 2016–2020. The NIS is the largest publicly available all-payer inpatient healthcare database in the United States and contains a stratified sample of hospital discharges from all HCUP-participating states, representing more than 95% of the US population (HCUP, 2025). The study population includes all patients hospitalized with a bicycling-related injury, identified using external cause of injury codes (E-codes V10-V19).

Variables and Measures

Demographics: Age, sex, race/ethnicity, income quartile, and insurance status.

Injury Characteristics: Motor vehicle involvement (MVC vs. non-MVC), transfer status, admission day (weekend vs. weekday), and injury severity measured by validated scoring systems, New Injury Severity Score (NISS), and Revised Injury Severity Score (RISS).

Geographic Classification: Patient home location was used as a proxy for crash location, categorized as urban or rural based on the National Center for Health Statistics (NCHS) classification, with rural areas defined as those with populations under 50,000.

Hospital Characteristics: Bed size, region (Northeast, Midwest, South, West), location (urban vs. rural), length of stay, and total hospital charges.

Outcome: Discharge disposition (routine, non-routine, death).

Statistical Analysis

Descriptive statistics summarized patient demographics, injury characteristics, and outcome by rural–urban residence. Chi-square tests were used to assess differences between strata. National estimates were calculated using NIS discharge weights and accounted for the dataset’s complex sampling design, including stratification, clustering, and weighting. All analyses were conducted in SAS 9.4.

RESULTS

Between 2016 and 2020, an estimated 124,000 inpatient hospitalizations for bicycle-related injuries occurred in the United States, with variations by year, demographic group, crash mechanism, and geography. The overall number of hospitalizations remained relatively stable from 2016 to 2019 but increased by approximately 5% in 2020.

Adults aged 51–70 years accounted for the largest proportion of hospitalizations (over 40%), followed by those aged 31–50 (25%). Across all age groups, males comprised approximately 80% of hospitalized patients, four times the number of females. While male injuries predominated in both rural and urban areas, female hospitalizations were more concentrated in urban settings. In rural areas, children and adolescents (<19 years) represented a greater share of hospitalized bicyclists compared to urban settings.

The crash mechanism analysis showed that nearly 80% of hospitalizations involved non–motor vehicle incidents, a pattern consistent across geographic regions. Most injuries occurred on weekdays, and white patients comprised the majority of hospitalized patients in both urban and rural areas (71%). The South and West U.S. census regions together accounted for nearly two-thirds of all hospitalizations, indicating regional clustering of injury burden.

More than 90% of bicycle-related hospital admissions occurred in urban areas. Although less frequent, injuries in rural settings were associated with slightly higher injury severity scores compared to those in urban areas. Of all hospitalized patients, 68.8% were discharged routinely to home, 29.8% had non-routine discharges such as transfers to skilled nursing facilities or home health services, and 1.4% died during hospitalization.

DISCUSSION

The findings of this analysis highlight substantial variation in bicycling injury hospitalizations across demographic and geographic groups in the United States. The increase in hospitalizations in 2020 may reflect changes in mobility patterns during the early phase of the COVID-19 pandemic, when cycling rose as a safer alternative to public transportation and a socially distanced recreational activity (Navon, 2023). Patterns suggest that injury burden is shaped by a

combination of age, sex, location, and crash context. Notably, non–motor vehicle incidents accounted for the majority of injuries, underscoring the importance of single crashes often overlooked in traditional road safety discussions. Regional and rural–urban differences in injury severity and hospital disposition point to broader disparities in healthcare access, cycling environments, and availability of proper infrastructure. Limited protected bike lanes, poor road surfaces, and longer distances to advanced medical care in certain areas may all contribute to the observed patterns. These contextual factors shape not only the likelihood of injury but also the type and outcome of medical care received.

Interpretation of these patterns is limited by the absence of exposure data, such as bicycling frequency or distance traveled by subpopulation. Without such data, differences by age, sex, or geography cannot be fully attributed to risk, as they may instead reflect differences in bicycling behavior or infrastructure. Nonetheless, the observed distributions offer important insight into where and for whom the greatest hospitalization burdens occur, with implications for targeted prevention, infrastructure planning, and healthcare system development.

CONCLUSION

Bicycling injury hospitalizations in the U.S. demonstrate clear differences across rural and urban settings, with distinct age patterns, injury severity, and care trajectories. While urban areas accounted for the majority of hospitalizations, rural regions showed greater representation among youth and slightly higher injury severity. The predominance of non–motor vehicle incidents across both settings underscores the importance of addressing infrastructure-related risks beyond motor vehicle conflicts. To inform effective, context-specific prevention strategies, future research should incorporate exposure data and account for geographic disparities in environmental and healthcare resources.

NOVELTY/TRAFFIC SAFETY IMPLICATIONS

This study offers one of the first national-level assessments of inpatient bicycling injuries stratified by rural–urban residence, identifying clear differences in age distribution, injury severity, and care outcomes. The predominance of non–motor vehicle crashes highlight the need for safety strategies beyond motorist conflict zones, including improved road surfaces, separated bike infrastructure, and rural-specific interventions. These findings support a broader public health approach to bicyclist injury prevention and inform geographically tailored infrastructure planning and resource allocation to reduce crash-related morbidity.

ACKNOWLEDGEMENTS

This research was supported by the H. Clay Gabler Scholar's Program Award from the Association for the Advancement of Automotive Medicine (AAAM).

REFERENCES

1. Centers for Disease Control and Prevention (CDC). (2022). *Web-based injury statistics query and reporting system (WISQARS)*. National Center for Injury Prevention and Control. Retrieved 03 from <https://wisqars.cdc.gov/>
2. Hamann, C., Peek-Asa, C., Lynch, C. F., Ramirez, M., & Torner, J. (2013). Burden of hospitalizations for bicycling injuries by motor vehicle involvement: United States, 2002 to 2009. *Journal of trauma and acute care surgery*, 75(5), 870-876.
3. Healthcare Cost and Utilization Project (HCUP). (2025). *HCUP Databases*. Agency for Healthcare Research and Quality. Retrieved February from www.hcup-us.ahrq.gov/nisoverview.jsp
4. McGuckin, N., & Fucci, A. (2018). *Summary of travel trends: 2017 national household travel survey*.
5. Mueller, N., Rojas-Rueda, D., Cole-Hunter, T., De Nazelle, A., Dons, E., Gerike, R., Götschi, T., Panis, L. I., Kahlmeier, S., & Nieuwenhuijsen, M. (2015). Health impact assessment of active transportation: a systematic review. *Preventive medicine*, 76, 103-114.
6. Næss, I., Galteland, P., Skaga, N. O., Eken, T., Helseth, E., & Ramm-Petersen, J. (2020). The number of patients hospitalized with bicycle injuries is increasing—A cry for better road safety. *Accident Analysis & Prevention*, 148, 105836.
7. Navon, L. (2023). Notes from the Field: Emergency Department Visits for Nonfatal Pedal Cyclist Injuries Before and During the COVID-19 Pandemic, United States, 2019–2020. *MMWR. Morbidity and Mortality Weekly Report*, 72.
8. PeopleForBikes. (2022). *Bicycling Participation Study: A survey of US residents*. https://prismic-io.s3.amazonaws.com/peopleforbikes/22d4a9f5-f114-4c5e-a40d-a32c7fa1567f_2022+PeopleForBikes+US+Bicycling+Participation+Study.pdf
9. Sarmiento, K., Haileyesus, T., Waltzman, D., & Daugherty, J. (2021). Emergency Department Visits for Bicycle-Related Traumatic Brain Injuries Among Children and Adults - United States, 2009-2018. *MMWR Morb Mortal Wkly Rep*, 70(19), 693-697. <https://doi.org/10.15585/mmwr.mm7019a1>

Evaluating Alcohol-Impairment in a Closed-Track Driving Study

Sparsh Jain and Miguel Perez, Ph.D.
Virginia Polytechnic and State University

INTRODUCTION

Alcohol-impaired driving remains a leading cause of motor vehicle crashes, injuries, and fatalities (Romano et al., 2018). While alcohol's effects on driving behavior are well-documented, most detection methods rely on observable vehicle control errors or delayed driver responses, limiting their effectiveness for early intervention (Lee et al., 2011). Physiological signals, such as heart rate (HR), respiration rate (RR), and neural activity (EEG), offer a potential alternative for detecting impairment before driving performance visibly declines. However, few studies have combined wearable sensing with alcohol dosing in an operational vehicle setting beyond laboratory or simulators (Chen, 2017).

This pilot study evaluated the feasibility and utility of wearable physiological sensors for detecting alcohol-induced changes during controlled experimental driving on a test track. Specifically, it examined sensor performance, quantified alcohol effects on physiology and driving metrics, and explored the potential of physiology-based impairment detection.

METHODS

This study recruited healthy adult drivers between the ages of 25-55 years with routine alcohol consumption to complete a controlled alcohol-dosing driving experiment at the Virginia Smart Roads closed test track. Participants drove a modified 2018 Ford Edge SE with rear seat safety controls and instrumented with an in-house data acquisition system and sensor suite, enabling full capture of vehicle dynamics, driver inputs, and six synchronized video views including forward roadway and face. Three wearable sensors recorded physiology throughout the session: Polar H10 (cardiac activity), DSI RESP Belt (respiration), and DSI-24 EEG headset (neural activity). Data was wirelessly streamed, time-synchronized with vehicle data, and processed for quality control.

Participants completed a baseline (sober) drive, an alcohol dosing session targeting 0.08% breath alcohol concentration (BrAC), and an impaired drive on the same course. The fixed route included urban-style segments with 25 mph speed limit and stop signs, turns, and roundabouts, along with a highway segment with 35 mph speed limit that encompassed

straight driving, lane changes, traffic light braking, and a 360° turnaround ramp. Alcohol dosing followed NIAAA guidelines using vodka mixed with juice, with continuous BrAC monitoring. Reaction time tests were completed in-lab before each drive, and a post-drive survey assessing perceived impairment and reactions to in-vehicle alcohol warnings followed the impaired session.

Data Analysis

Driving data was segmented into six maneuver types and a 5-minute steady-state "quiet" period. Key metrics included steering, speed, lane position variability (SDLP), reaction time, and eye closure. Physiological features (i.e., HR, RR, heart rate variability (HRV), respiratory rate variability (RRV), EEG power in delta, theta, alpha, beta, and gamma bands) were extracted per segment. Within-subjects statistical comparisons (Baseline vs. Impaired) used generalized linear models (GLM) with participant as a random effect ($\alpha=0.05$).

RESULTS

Five participants (three male, two female; ages 27-46 years) completed all study procedures. Sensor reliability varied by modality. The Polar H10 chest strap provided consistently high-quality ECG signals with minimal artifact. The respiration belt performed adequately, though signal quality was sensitive to belt fit and posture. EEG data collection proved the most challenging, with frequent motion artifacts requiring extensive cleaning and manual rejection of noisy segments. Despite these challenges, meaningful EEG metrics were recoverable in most sessions.

Reaction Time

Alcohol consumption slowed reaction times in both tasks. Lab-based reaction time increased from 224 ms to 246 ms ($p = 0.013$), while on-road braking reaction time increased from 1021 ms to 1372 ms, though the differences were not statistically significant.

Driving Performance

Alcohol impairment produced measurable changes in several aspects of driving behavior (as shown in Table 1), particularly in steering control, speed maintenance, and lateral position variability. The clearest effects were observed during straight driving maneuvers (downhill and uphill), where steering angles increased significantly (mean increase of 0.4°,

$p = 0.01$), alongside higher steering variability and greater speed. Eye closure proportion, an indicator of reduced alertness, also increased notably in straight segments (up to +9.8%).

Curved driving maneuvers, including roundabouts and highway ramps, showed increased steering angles, higher yaw rate variability, and elevated speeds. Specifically, during the highway ramp maneuver, mean speed increased by 2.4 miles per hour (mph) ($p = 0.045$), and standard deviation of lateral position (SDLP) increased by 4.3 cm. In contrast, the lane change maneuver did not show consistent impairment-related effects.

Table 1. Summary of Driving Performance Changes (Impaired – Baseline)

| Segment | Metric | Direction | Difference |
|------------|---------------------|-----------------|-------------|
| Downhill | Mean steering angle | ↑ ($p=0.01$) | +0.4° |
| | Steering angle SD | ↑ | +0.07° |
| | Eye closure | ↑ | +9.8% |
| | Mean speed | ↑ | +1.4 mph |
| | Min speed | ↑ | +2.0 mph |
| | Max speed | ↑ | +2.3 mph |
| | Speed SD | ↓ | -0.13 mph |
| | SDLP | ↑ ($p=0.09$) | +2.27 cm |
| | Longitudinal acc SD | ↑ | +0.010 g |
| Uphill | Mean steering angle | ↑ ($p=0.001$) | +0.4° |
| | Steering angle SD | ↑ | +0.25° |
| | Eye closure | ↑ | +3.3% |
| | Mean speed | ↑ | +1.0 mph |
| | Min speed | ↓ | -1.3 mph |
| | Max speed | ↑ | +1.9 mph |
| | Speed SD | ↑ | +0.72 mph |
| | SDLP | ↓ | -2.08 cm |
| | Longitudinal acc SD | ↑ | +0.010 g |
| Roundabout | Mean steering angle | ↑ | +3.0° |
| | Steering angle SD | ↑ | +0.9° |
| | Mean speed | ↑ | +0.3 mph |
| | Speed SD | ↑ | +0.1 mph |
| | Yaw rate SD | ↑ ($p=0.06$) | +0.9 deg/s |
| Ramp | Mean steering angle | ↑ | +0.35° |
| | Steering angle SD | ↑ | +0.08° |
| | Yaw rate | ↑ | +0.85 deg/s |
| | Mean speed | ↑ ($p=0.04$) | +2.4 mph |
| | Speed SD | ↑ ($p=0.06$) | +0.47 mph |
| | SDLP | ↑ | +4.28 cm |

Physiological Outcomes

HR increased significantly across all participants following alcohol consumption, rising from a baseline mean of 69.5 beats per minute (bpm) to 83.0 bpm under impairment ($p = 0.017$). Consistent with elevated sympathetic activation, heart rate variability (HRV) decreased, with the mean NN interval dropping by approximately 150 ms ($p = 0.027$). Long-term HRV (SDANN1) also declined, although this metric did not reach significance ($p = 0.08$). RR decreased from 24.3 to 21.6 breaths per minute (brpm), accompanied by a reduction in respiratory volume per time (-18%). At the same time, measures of respiratory variability (i.e., RMSSD, SD2/SD1 ratio) increased, indicating more irregular breathing patterns. Both inspiration and expiration durations lengthened during impairment, reflecting slower breathing cycles.

EEG analysis revealed subtle increases in relative alpha power (+6%), with a reduction in the dominant alpha frequency from 10.7 Hz to 9.6 Hz, suggesting cortical slowing. Frontal theta power increased regionally, though overall theta power declined slightly (-1%). Only small power increases were observed in beta and gamma bands (+1%).

Behavioral Responses

Participants poorly estimated their own BrAC (mean error = 0.016%, ~20% of range), with both over- and under-estimation observed. Most acknowledged feeling too impaired to drive but were uncertain about exceeding the legal limit. The willingness to drive while impaired was mixed, with responses clustering near neutral. When hypothetically presented with an in-vehicle alcohol warning, most preferred calling an Uber, though attitudes toward ignition interlock systems ranged from full support to passive or conditional acceptance.

DISCUSSION

This study demonstrated that wearable physiological sensors can capture alcohol-related changes during real vehicle operation, extending prior laboratory findings into a real-vehicle dynamic driving context. ECG signals were consistently reliable, in line with past research on chest-strap monitors in active settings (Scardulla et al., 2020). Respiration signals were generally usable with minor adjustments, while EEG data remained the most sensitive to motion artifacts- a well-documented challenge in mobile EEG studies (Fedotov et al., 2018; Puce & Hämäläinen, 2017). Physiological responses aligned with known alcohol effects, including elevated heart rate, reduced heart rate variability, slightly slower breathing, and increased respiratory variability. EEG changes were smaller but consistent with prior

alcohol research, showing increased alpha power and decreased peak alpha frequency (Tran et al., 2004; Van De Borne et al., 1997). Driving performance changes were modest but directionally consistent with existing simulator and on-road studies, including increased steering variability, SDLP, speed, and slower reaction times (Simmons et al., 2022).

While this study used real driving on a closed test track, it does not fully replicate the variability or complexity of naturalistic driving. The small sample size (n=5), variable EEG quality, and fixed drive order further limit generalizability. Future work should scale this approach to larger, more diverse samples in on-road environments, while improving wearable EEG hardware, artifact rejection techniques, and integrated multi-sensor analytics for in-vehicle impairment detection.

CONCLUSION

This study demonstrated that wearable physiological sensors can capture meaningful indicators of alcohol impairment during real-world driving on a closed test track. Alcohol consumption increased heart rate, slowed breathing, reduced heart rate variability, and altered EEG activity, alongside measurable changes in driving behavior such as increased steering variability, lane deviation, and slower reaction times.

While ECG and respiration sensors performed reliably, EEG data collection in a moving vehicle remained challenging but feasible with careful processing. Integrating physiological monitoring with traditional driving metrics offers a promising path for future in-vehicle impairment detection systems but will require further research to overcome technical and practical challenges in real-world applications.

NOVELTY/TRAFFIC SAFETY IMPLICATIONS

Very few studies globally have combined controlled alcohol dosing with real driving, and almost none have integrated wearable physiological monitoring in an operational vehicle. This study is among the first in North America to collect synchronized cardiac, respiratory, and neural data during alcohol-impaired driving on a closed test track.

Physiological sensing offers the potential to detect impairment earlier than traditional behavior-based systems, capturing internal changes before visible driving errors occur. Integrating these signals into future driver monitoring technologies could enable earlier warnings or intervention, reducing alcohol-related crashes, injuries, and fatalities by preventing impaired driving before critical mistakes happen.

This experimental framework also provides a model for evaluating future impairment detection technologies as sensing hardware improves and more unobtrusive physiological monitoring becomes feasible in production vehicles.

ACKNOWLEDGEMENTS

This study was funded by the National Surface Transportation Safety Center for Excellence (NSTSC) and Responsibility.Org. The authors thank Dr. Ashley Brooks-Russell, Dr. Tim Brown, Dr. Naomi Dunn, VTTI's Hardware Engineering Lab (HEL), and the research team for their support.

REFERENCES

- Fedotov, A., Akulov, S., & Akulova, A. (2018). Motion artifacts reduction in wearable respiratory monitoring device. *EMBEC & NBC 2017*
- Lee, J., Brown, T., Fiorentino, D., Fell, J. C., Nadler, E., & John, A. (2011). Using vehicle-based sensors of driver behavior to detect alcohol impairment.
- Puce, A., & Hämäläinen, M. S. (2017). A review of issues related to data acquisition and analysis in EEG/MEG studies. *Brain sciences*, 7(6), 58.
- Romano, E., Torres-Saavedra, P. A., Calderón Cartagena, H. I., Voas, R. B., & Ramírez, A. (2018). Alcohol-related risk of driver fatalities in motor vehicle crashes: comparing data from 2007 and 2013–2014. *Journal of studies on alcohol and drugs*, 79(4), 547-552.
- Scardulla, F., D'Acquisto, L., Hu, S., Pasta, S., & Bellavia, D. (2020). A study on the effect of contact pressure during physical activity on PPG heart rate measurements. *Sensors*, 20(18), 5052.
- Simmons, S. M., Caird, J. K., Sterzer, F., & Asbridge, M. (2022). The effects of cannabis and alcohol on driving performance and driver behaviour. *Addiction*, 117(7), 1843-1856.
- Tran, Y., Craig, A., & Nicholson, G. (2004). Time course and regional distribution of cortical changes during acute alcohol ingestion. *International journal of neuroscience*, 114(7), 863-878.
- Van De Borne, P., Mark, A. L., Mion, D., & Somers, V. K. (1997). Effects of alcohol on sympathetic activity, hemodynamics, and chemoreflex sensitivity. *Hypertension*, 29(6), 1278-1283.

Human Cervical Intervertebral Disc Pressure Response in Compressive Impacts: Methodology & Initial Results

Sara Sochor

MOBIOS Lab, Comillas Pontifical University, Madrid, Spain

Mark R. Sochor, Juan M. Asensio-Gil, Carlos Rodríguez-Morcillo García, & Francisco J. López Valdés

INTRODUCTION

Cervical spine injuries are a notable concern in motor vehicle collisions (MVCs), and ongoing advancements in vehicle safety technology and injury prediction and prevention tools continue to play a crucial role in reducing their prevalence and severity. Human surrogates for injury biomechanics testing (anthropometric test devices (ATDs), i.e., “crash test dummies” and computational models, i.e., Human Body Models (HBMs)) must closely mimic human physical characteristics to ensure the surrogate mechanical responses simulate comparable human responses (Mertz, 2002; Yoganandan et al., 2015). While human surrogates exhibit a distinct set of intrinsic advantages and disadvantages (Crandall et al., 2011), the actual human body tolerance falls somewhere between the investigative capacities of both ATDs and HBMs. There is a paucity of data for cervical intervertebral disc (IVD) tissue response, yet there are positive implications for understanding IVD response as it relates to overall cervical spine kinematics, especially for more widespread application to injury biomechanics. Cervical IVD tissue response data could be utilized to assess and supplement the characterization of the head-neck complex to failure, and resultant data could facilitate the continued improvement of both ATDs and HBMs.

Previous studies have attempted to establish a relationship between cervical IVD pressures and cervical spine motion/loading (Hattori et al., 1981; Pospiech et al., 1999; Cripton et al., 2001); however, to date, the exact relationship of cervical IVD pressures to loading is still uncertain and is the focus of this research. To investigate the potential applicability of cervical IVD pressures to cervical spine injury tolerance, we replicated the hallmark human cervical spine injury biomechanics experimentation conducted by Nightingale et al. (Nightingale et al., 1996, 1997) with the addition of novel cervical IVD pressure sensor instrumentation. To our knowledge, implanting pressure sensors into the cervical IVDs of component PMHS (i.e., cephalus with spine) has not been previously reported in the

biomechanics literature. This feasibility study describes a methodology to evaluate the potential of cervical IVD pressure sensors in detecting injurious compressive load on PMHS head-cervical spine specimens.

METHODS

Experimental System

As in the Nightingale studies (Nightingale et al., 1996, 1997), a vertical drop test system was designed to simulate an axial head impact with a following torso load, while controlling for initial PMHS positioning, drop height, and impact surface orientation (**Figure 1**).

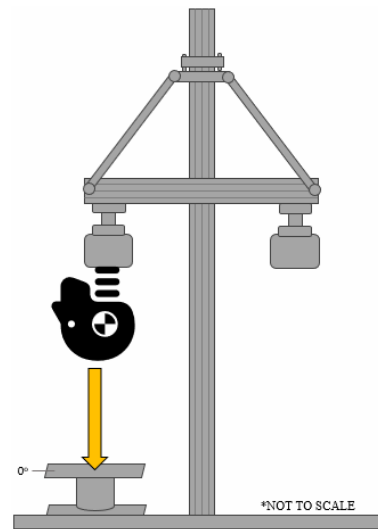


Figure 1. Vertical drop test system designed to replicate cervical spine experimentation conducted by Nightingale et al. (1996, 1997).

The vertical drop tower (Ibertest; Madrid, ES) was comprised of two linear rails with bushing sliders and the total carriage and counterweight aimed to approximate the weight of a fiftieth percentile male upper torso mass (~16 kg) (Nightingale et al., 1996, 1997). The impact surface consisted of a Teflon covered steel plate positioned under the PMHS skull apex to simulate a rigid unconstrained vertex (0°) head

impact. A six-axis load cell was installed at each end of the test apparatus (MC3A-1000 & MC5-10000; AMTI, Watertown, MA, USA). Kinematic and pressure data were coordinated and acquired at sample rate of 1,000 Hz and 20,000 Hz respectively. A digital data acquisition system (DAS) (DTS Slice Micro with DataPRO software; DTS, Seal Beach, CA, USA) recorded data from the accelerometer and pressure sensors, and a 3D motion capture system (Vicon Motion System; Kidlington, UK) recorded specimen kinematics. Experiments were imaged at 2,000 frames per second (FASTCAM SA3; Photron, Bucks, UK). Data analysis was performed in BETA CAE META (Version: 24.0.1, Davos-Platz, CH).

Specimen Preparation

Four fresh frozen male component head-neck PMHS (i.e., cephalus with spine through the fourth thoracic vertebrae (T4)) were tested in accordance with the ethical guidelines established by the Human Usage Review Panel of the National Highway Traffic Safety Administration (NHTSA). Three of the four subjects were deemed to have healthy cervical vertebrae and intervertebral discs with limited (age appropriate) degeneration, while one specimen exhibited tissue degradation related to clinical treatment and thus acted as an experimental pilot. Limited soft tissue was removed from the PMHS to maintain natural anatomical influence of surrounding structures. The three caudal-most thoracic vertebrae (T2-T4) were denuded and potted in an aluminum cup with ultra-low viscosity casting resin, taking care to maintain the neutral first thoracic vertebrae (T1) angle (25°) (Matsushita et al., 1994) and to ensure the C7/T1 motion segment was not hindered by the potting material. Each PMHS was instrumented with miniature pressure sensors at multiple cervical IVD levels (Model 060S; Precision Measurement Company, Ann Arbor, MI, USA) using a minimally invasive surgical technique. 3D motion tracking arrays were installed anteriorly at multiple cervical vertebral levels, and a six degree-of-freedom sensor package (6DX PRO-A 500G; DTS, Seal Beach, CA, USA), was installed on the lateral skull parallel to the Frankfurt plane. PMHS underwent post-instrumentation CT to confirm both instrumentation placement and the neutral T1 potted angle of ~25°.

Test Protocol

Specimen positioning was performed to replicate and facilitate comparison with previous Nightingale tests (Nightingale et al., 1996, 1997). Potted PMHS were placed in an inverted neutral head/neck posture (i.e., Frankfurt horizontal plane parallel to the ground), thus preserving natural resting cervical lordosis. The magnitude of applied displacement was scaled based on a specimen length ratio, as in a previous Nightingale study (Nightingale et al., 1991), to

calculate specimen-specific axial deflection limits (i.e., stroke). Specimens were raised to the drop height of 0.53 meter in order to reach the desired impact velocity of ~3.2 m/s. The PMHS were released and allowed to drop vertically, sustaining impact with the load plate below. Post-test CT imaging and subsequent dissection determined the extent of injury sustained.

RESULTS

Two of the four PMHS generated viable test data, in which cervical kinematics and IVD pressure readings were successfully obtained for all instrumented spine levels. Characteristic cervical spine deformations/buckling motion patterns upon head impact were observed. Marked IVD pressure differences were noted between the cervical levels assessed, and there was successful repeatability between the tests. Both PMHS exhibited similarly shaped pressure peaks despite slightly different IVD instrumentation levels. The more cranial (C2-C4) and caudal (C6-T1) IVD levels exhibited greater and more comparable pressure values than those of the mid-spine disc level (C4-C6), and the average pressure in upper/lower levels was ~50 times higher than that of the middle (**Table 1**).

Table 1. Summary of absolute pressure value and axial head/neck force means.

| Absolute Pressure (PSI) | | | Force (N) | |
|-------------------------|-------|-------|-----------|--------|
| C2-C4 | C4-C6 | C6-T1 | Head Z | Neck Z |
| 359.8 | 6.9 | 334.0 | 4730.4 | 1730.5 |
| +/- | +/- | +/- | +/- | +/- |
| 124.9 | 8.3 | 51.6 | 1297.9 | 28.3 |

The average peak axial neck force was comparable to previous Nightingale studies (Nightingale et al., 1996, 1997) (**Table 1**), as were the resultant cervical spine injuries. Radiographic post-test imaging identified positive cervical spine injury. One PMHS sustained a type II Jefferson (C1) fracture and a C3 vertebral body fracture, while the other PMHS displayed a type 3 dens (C2) fracture.

DISCUSSION

The results of this study proved very compelling. To our knowledge, this is the first study to implement the use of miniature pressure sensors in component PMHS cervical spine IVDs to assess pressure changes during injurious biomechanical cervical spine testing. These results show that cervical IVD pressures can potentially be used to assess injurious events in axial compression of the cervical spine. Limitations were observed in this study. The “oversimplification” of a one-degree-of-freedom (i.e., vertical only) experimental protocol using isolated PMHS

components (versus whole body PMHS) is often considered a limitation (Kerrigan et al., 2014); however, we feel that this preliminary approach best correlates the results of previous work with the application of novel instrumentation. Variations in sensor positioning within the PMHS cervical IVD may have affected the recorded pressure outputs. Plans for sensor placement improvement utilizing patient-specific CT scans have been established for future testing.

CONCLUSION

This study was an initial step in determining the potential applicability of cervical IVD pressures to assess the axial compression injury tolerance of the human cervical spine. While still limited in terms of exact values, the recorded pressures provide valuable information regarding cervical IVD pressure curve timing, rates of pressure increase, and peak pressures relative to specimen kinematics and other experimental parameters.

NOVELTY/TRAFFIC SAFETY IMPLICATIONS

Ongoing research into MVC related cervical spine injuries contributes to the development of innovative safety technologies and crash prevention systems, injury countermeasures, and the design of proper human surrogates (i.e., ATDs/HMBs).

ACKNOWLEDGEMENTS

We would like to acknowledge all the personnel at our laboratory who provided their assistance and expertise in the execution and analysis of these experiments, as well as the hospitality of Drs. R. Nightingale and J. Luck at Duke University. And lastly, for the altruistic gift of donor bodies, without which our research would not be possible.

REFERENCES

Crandall, J. R., Bose, D., Forman, J., Untaroiu, C. D., Arregui-Dalmases, C., Shaw, C. G., & Kerrigan, J. R. (2011). Human surrogates for injury biomechanics research. *Clinical Anatomy*, 24(3), 362–371. <https://doi.org/10.1002/ca.21152>

Cripton, P. A., Dumas, G. A., & Nolte, L.-P. (2001). A minimally disruptive technique for measuring intervertebral disc pressure in vitro: Application to the cervical spine. *Journal of Biomechanics*, 34(4), 545–549. [https://doi.org/10.1016/S0021-9290\(00\)00205-0](https://doi.org/10.1016/S0021-9290(00)00205-0)

Hattori, S., Oda, H., & Kawaii, S. (1981). Cervical intradiscal pressure in movements and traction of the cervical spine. *Z Orthop*, 119, 568–569.

Kerrigan, J. R., Foster, J. B., Sochor, M., Forman, J., Toczyski, J., Roberts, C. W., & Crandall, J. R. (2014). Axial Compression Injury Tolerance of the Cervical Spine: Initial Results. *Traffic Injury Prevention*, 15(sup1), S238–S269. <https://doi.org/10.1080/15389588.2014.956646>

Matsushita, T., Sato, T. B., Hirabayashi, K., Fujimura, S., Asazuma, T., & Takatori, T. (1994). X-Ray Study of the Human Neck Motion Due to Head Inertia Loading. *SAE Transactions*, 103, 1623–1632.

Mertz, H. J. (2002). Anthropomorphic Test Devices. In A. M. Nahum & J. W. Melvin (Eds.), *Accidental Injury: Biomechanics and Prevention* (pp. 72–88). Springer. https://doi.org/10.1007/978-0-387-21787-1_4

Nightingale, R. W., Doherty, B. J., Myers, B. S., McElhaney, J. H., & Richardson, W. J. (1991). The Influence of End Condition on Human Cervical Spine Injury Mechanisms. *SAE Transactions*, 100, 2040–2048.

Nightingale, R. W., McElhaney, J. H., Camacho, D. L., Kleinberger, M., Winkelstein, B. A., & Myers, B. S. (1997). The Dynamic Responses of the Cervical Spine: Buckling, End Conditions, and Tolerance in Compressive Impacts. *SAE Transactions*, 106, 3968–3988. JSTOR.

Nightingale, R. W., McElhaney, J. H., Richardson, W. J., Best, T. M., & Myers, B. S. (1996). Experimental Impact Injury to the Cervical Spine: Relating Motion of the Head and the Mechanism of Injury. *The Journal of Bone and Joint Surgery*, 78(3).

Pospiech, J., Stolke, D., Wilke, H. J., & Claes, L. E. (1999). Intradiscal pressure recordings in the cervical spine. *Neurosurgery*, 44(2), 379–384; discussion 384–385. <https://doi.org/10.1097/00006123-199902000-00078>

Yoganandan, N., Nahum, A. M., Melvin, J. W., & The Medical College of Wisconsin Inc on behalf of Narayan Yoganandan (Eds.). (2015). *Accidental Injury: Biomechanics and Prevention*. Springer New York. <https://doi.org/10.1007/978-1-4939-1732-7>